IEEE Photonics Journal
An IEEE Photonics Society Publication

Open Access

# Stacked Encapsulation Structure for Discretely Distributed Quantum Dot Array

Volume 12, Number 2, April 2020

Jing Cai
Jianyao Lin
Yu Chen
Sheng Xu
Yun Ye
Enguo Chen
Tailiang Guo

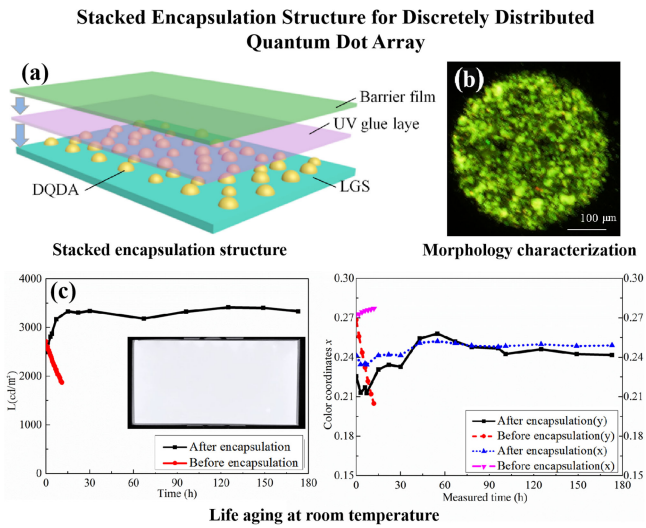


DOI: 10.1109/JPHOT.2020.2977218

# Stacked Encapsulation Structure for Discretely Distributed Quantum Dot Array

**Jing Cai, Jianyao Lin, Yu Chen, Sheng Xu, Yun Ye, Enguo Chen, and Tailiang Guo**

National & Local United Engineer Laboratory of Flat Panel Display Technology, College of Physics and Information Engineering, Fuzhou University, Fuzhou 350116, China

*DOI:10.1109/JPHOT.2020.2977218*


Manuscript received February 15, 2020; accepted February 25, 2020. Date of publication February 28, 2020; date of current version March 11, 2020. This work was supported in part by National Key Research and Development Plan under Grant 2017YFB0404604, and in part by Fujian Science and Technology Key Project under Grant 2018H6011. Corresponding authors: Enguo Chen; Tailiang Guo (e-mail: ceg@fzu.edu.cn; gtl_fzu@hotmail.com).

**Abstract:** The performances of quantum-dot (QD) based photoluminescent devices are highly restricted by the application environment, especially the moisture and oxygen. However, current external encapsulation structures are not applicable to the devices with discrete QD distribution, especially for some rough profiles. To address this issue, an encapsulation method for discretely distributed quantum-dot arrays (DQDA) is proposed for liquid crystal display (LCD) backlight applications, in which the DQDA can be well fabricated by printing the QD slurry onto a light guiding substrate (LGS), and then covered with a thin UV glue layer and a barrier film. By specially optimizing the UV glue and barrier film, this ultra-thin encapsulation structure cannot only improve the surface defects of the QD morphology without affecting the original light path and the output optical performance, but also significantly suppress the fluorescence decay and isolate moisture and oxygen by almost 100 times compared with unencapsulated one. The water vapor transmission rate (WVTR) was measured to be $1.29 \times 10^{-4}$ g/m$^2$/day after fabricated the stacked encapsulation structure. After a long period of aging test, the encapsulated sample kept its luminance for 1000 hours. This method also has potential to widely used for discrete structures in other device applications due to its easy fabrication process, high reliability, and low manufacturing costs.

**Index Terms:** Quantum-dot array, moisture, oxygen, encapsulation, stacked structure.

## 1. Introduction

Quantum dots (QDs) [1], [2], a kind of advanced nano-materials, have received widespread attention because of their unique photoelectric properties, narrow half peak width, and tunable color, characterized by high color purity and color gamut. The luminescence and color characteristics of QD-enhanced LCD backlights [3]–[8] can surpass traditional LED backlight using phosphors as light converters [9]–[11], which are comparable to organic light-emitting diode (OLED) [12], [13]. Although QD based devices are less sensitive to moisture vapor and oxygen than OLED devices [14]–[16], they are still easy to lose efficacy while directly exposed to oxygen and moisture. It is therefore necessary to develop effective encapsulation methods to improve the operation life of QD devices.

Current encapsulation methods for QD devices can be concluded into two categories: internal and external encapsulation. Internal encapsulation refers to a series of chemical actions, which

directly forms a protective layer on the QD surfaces [17]–[19]. For example, by simply doping Al into the shell of CdSe/CdS QDs, a dense alumina layer was oxidized and formed, which can maintain the original brightness after 24 hours of irradiation [20]. Jun [21] *et al.* replaced the oleic acid ligand on the surface of cadmium selenide/cadmium sulfide/zinc sulfide QDs with mercaptoethanol, and then used propylamine as a catalyst for silica sol-gel condensation to obtain hydrolyzate of mercaptoethanol and ethyl orthosilicate. The condensation-coated silica can retain original brightness of the encapsulated chip for 250 hours. Yoon [22] *et al.* proposed to use amino-linked methyl methacrylate to replace the original oleic acid ligand on the surface of CdSe/ZnS QDs, which can increase the conversion efficiency by 24%. Xie [23] *et al.* prepared a passivated Zn-PDMs precursor for in-situ QD synthesis to protect the QDs from reacting with impurities and maintain monodispersity. Although progresses on internal encapsulation methods have been achieved in laboratory environment, some technical barriers are still difficult to avoid in mass production [24]–[26]. Microscopically, it is hard to detect each QD encapsulated perfectly [27]. External encapsulation could provide a complementary solution. At present, there are three main external encapsulation approaches: on chip, on surface, and on edge. On-surface approach refers to an optical film made of QD material sandwiched in a thin film to generate uniform surface light [28]–[30]. On-edge type (QD tube or QD rail) [31] seals the QD fluorescent material into a thin glass tube for edge-lit backlight applications. On-chip solution, also known as “on chip” mode, encapsulates QD onto LED chips to fabricate chip beads [32]. For this kind of methods, a reasonable barrier layer is needed to prevent the small molecules of moisture vapor and oxygen from eroding the surface of QDs [33]–[36], that is, to encapsulate QD materials [37]–[42]. In summary, external encapsulation methods are more feasible and practical to operate in actual applications than internal ones. However, all of the present external encapsulation structure are not applicable to the devices with discrete quantum-dot distribution, especially for some rough profiles.

To address this issue, this paper proposes a novel external encapsulation method for DQDA, namely stacked encapsulation structure. The DQDA can be considered as a light extraction medium on a light guiding substrate printed by specially prepared QD slurry. After that, the DQDA is covered by a spin-coated UV glue layer and a barrier film to well block moisture and oxygen.

## 2. Materials and Methods

### *2.1 Encapsulation Structure*

The lifetime of the QD device is an indicator for their stability, and the encapsulation structure is the key technology to extend the lifetime. Encapsulation structures will greatly influence the device performance, and the encapsulation materials will have different effects on the uniformity and emission efficiency of the light output. At the beginning of the experiment, UV glue and barrier film are selected as the key encapsulation materials because of their near refractive index and strong ability to block moisture and oxygen. The UV glue (NEA121) and the barrier film (WS-130) were purchased from Boer Technology Co., Ltd.. The NEA121 is a kind of single-component adhesive liquid that can become an elastic polymer layer after curing. The commonly used thickness of the barrier film has two specifications, 130 $\mu$m and 50 $\mu$m. After testing, the former one has better barrier properties, and one surface is engraved with a series of nano structures for light homogenization. Therefore, the thickness of 130 $\mu$m was finally determined. This thin and flexible barrier film made of polyethylene terepythalate can be well attached to the UV glue layer to further improve encapsulation performance. As shown in the Fig. 1, the stacked structure includes three layers, where the bottom layer is a light guiding substrate (LGS) with printing DQDA for uniform light distribution in LCD backlights, the middle one is a UV glue layer, and the upper one is a barrier film.

### *2.2 Process of Fabricating the Calcium Film*

Water vapor transmission rate is an important index to reflect the device’s lifetime. Calcium corrosion method is a common approach to measure the water vapor transmission rate [43]. Since

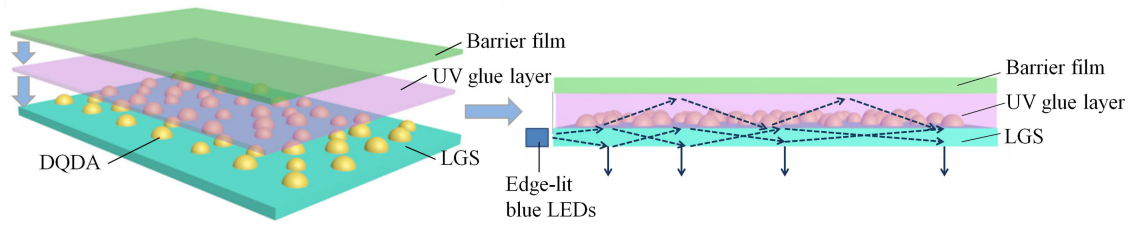


Fig. 1. The stacked encapsulation structure with the sandwiched DQDA.

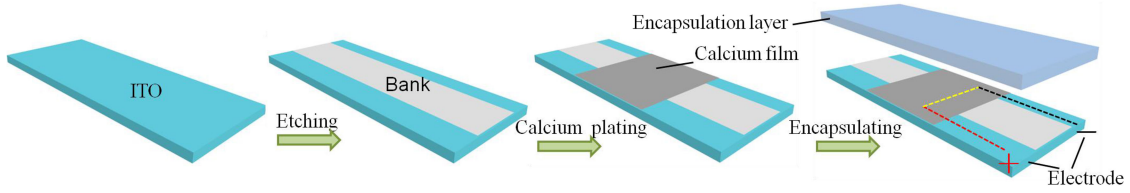


Fig. 2. The fabrication process of a calcium film for the calcium corrosion method.

calcium is extremely sensitive to moisture and oxygen, it is easily oxidized into a non-conductive oxide when exposed to air, and the encapsulation performance will be reflected by measuring the tendency of the resistance of the encapsulated calcium film. When fabricating a calcium film, the ITO glass was firstly cleaned, and then was successively placed in the glass washing liquid, acetone, absolute ethanol, and deionized water for ultrasonic cleaning 10 minutes, and finally was dried by using N2. The technological process of encapsulating a calcium film is shown in the Fig. 2. The micro electrode channels were firstly constructed on the ITO glass substrate by standard UV photolithography and wet etching technique. Then the calcium film was evaporated onto the channel under a nitrogen (N2) atmosphere. The thickness of the calcium film is about 200 nm. Finally, an encapsulation layer was fabricated onto the calcium film by firstly attaching the ITO glass on the spinning coater, and then spinning the UV glue on the glass evenly. The calcium film can be used as a bridge to connect the positive and negative electrodes. After the calcium film was completely corroded, calcium oxide and calcium hydroxide were generated and resulted in a non-conducting bridge.

### *2.3 Water Vapor Transmission Rate (WVTR) After Encapsulation*

The capability of isolating moisture and oxygen is evaluated to verify the stacked encapsulation structure. As an important indicator of lifetime, the WVTR mentioned above can directly reflect whether the moisture and oxygen are isolated effectively. Here, the WVTR of stacked encapsulation method was measured by the calcium corrosion method described above. Since high transmittance is required for backlights, two experimental groups were set here for comparison. In the first group, the spinning coater was accelerated to reach the set speed in 10 seconds, and then kept for 30 seconds at a constant speed. The UV glue was spin coated on pure glass pieces (2 cm $\times$ 2 cm) with speed of 300 RPM (revolutions per minute), 400 RPM, 500 RPM, 600 RPM, and 700 RPM, respectively. For another group, the barrier film was attached after the UV glue was spin coated in the same way above. After that, the two groups were placed under a UV curing lamp for curing 60 seconds. Finally, the blank glass was placed in the spectrophotometer (UV3600) for calibration, and then was tested one by one. The thickness of UV glue film is influenced by spin velocity and acceleration. The thicker the thickness is, the lower the transmittance of the glue layer is. The transmittances of the two groups are shown in Fig. 3.

From the perspective of transmittance, all UV glue layers in the first group almost reach 99% during the wavelength range from 400 nm to 800 nm, indicating that the selected glue provides

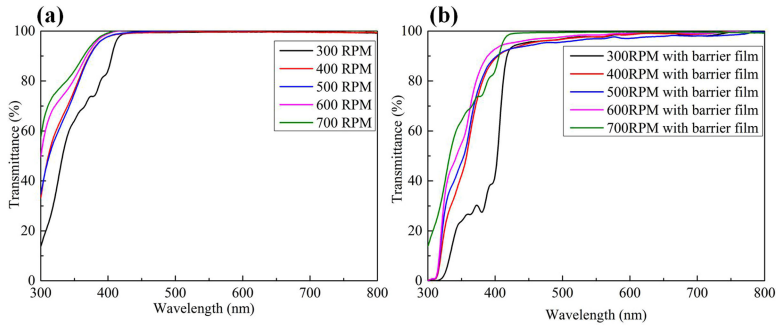


Fig. 3. Transmittance curves of the UV glue layer and the barrier film: (a) only a UV glue layer included. (b) both a UV glue layer and a barrier film included.

TABLE 1
Experimental Data of the UV Glue Layers Prepared by Different Spin-Coating Speeds

| Speed (RPM) | 300 | 400 | 500 | 600 | 700 |
|---|---|---|---|---|---|
| Thickness (μm) | 150.12 | 100.34 | 80.32 | 60.57 | 50.93 |
| Transmittance | 98.17% | 98.23% | 98.53% | 98.65% | 98.74% |
| WVTR (g/m$^2$/day) | 0.039 | 0.037 | 0.032 | 0.031 | 0.023 |

high transmittance and does not affect the light emission. For the second group, the transmittance decreases slightly because of the insertion of the barrier film. Even so, the transmittances of all layers are higher than 98%. High transmittance ensures the light extraction from the QD backlight.

Calcium corrosion method is designed for WVTR measurements in order to evaluate the encapsulation performance. The WVTR values were measured by using the ITO glasses with the calcium films. The UV glue layers with different thicknesses were obtained by spin-coating speeds at 300 RPM, 400 RPM, 500 RPM, 600 RPM, 700 RPM. After drying, these ITO glasses were attached to the positive and negative electrodes. The amount of water vapor permeating through the film can be estimated from the calcium corrosion according to the following formula:

$$\mathrm{WVTR}\,[\mathrm{g}/(\mathrm{m}^2 day)] = -n \times \delta_{\mathrm{Ca}} \times \rho_{\mathrm{Ca}} \times \frac{d(\frac{1}{R})}{dt} \times \frac{M(H_2O)}{M(Ca)} \times \frac{l}{b} \times \frac{\mathrm{Ca}_{\mathrm{Area}}}{\mathrm{Window}_{\mathrm{Area}}} \tag{1}$$

where, $n$ represents the molar ratio of the chemical reaction with the corrosion of calcium film. Since the resistance change of the film is caused by moisture and vapor permeation, $n = 2$ is generally taken for calculation. The conductivity and density of Ca are defined by $\delta_{\mathrm{Ca}} = 3.19 \times 10^{-8}\Omega{\cdot}\mathrm{m}$ and $\mathrm{p}_{\mathrm{Ca}} = 1.55$ g/cm$^3$, and the molar mass of $H_2O$ and Ca are $M(H_2O) = 18$ g/mol and $M(Ca) = 40$ g/mol, respectively. l and b are respectively the length and width of the prepared calcium films. 1/R was the measured resistivity. $\mathrm{Ca}_{\mathrm{Area}}$ is the effective test area. $\mathrm{Window}_{\mathrm{Area}}$ represents the window area of the mask. In this experiment, $\mathrm{Ca}_{\mathrm{Area}}/\mathrm{Window}_{\mathrm{Area}} = 1$. The specific values of thickness and WVTR are listed in Table 1. Among them, the thickness of UV glue layer was measured by a profilometer (Dektak-XT).

It can be found in Table 1 that the thickness change of the UV glue layer hardly affects the value of WVTR. In order to further study the encapsulation performance, the barrier film was bonded on the UV glue with 100 $\mu$m thickness and then tested by calcium corrosion method. Finally, WVTR $= 1.29 \times 10^{-4}$ (g/m$^2$/day) can be obtained by Eq. (1), which means the lifetime reaches above 1000 hours while converted into service life.

The WVTR significantly decreased after the barrier film was attached. The DQDA height on the LGS is about 20 $\mu$m. The height of the UV glue layer should be set by 5 times the DQDA height according to our previous experience, so that the thickness of the glue layer is about 100 $\mu$m. The

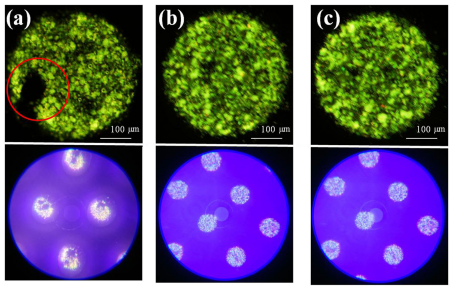


Fig. 4. Morphology of the DQDA: (a) dissolution between the glue layer and the DQDA layer. The morphology: (b) before and (c) after encapsulation by using UV glue processing.

scheme of 400 RPM with a barrier film attached has obvious advantages, and the barrier film is adhered to further improve the water-proof performance.

## 3. Experimental Results

### *3.1 Morphology Characterization and Optical Performance*

Based on the above analysis, the stacked encapsulation structure was applied to fabricate a photoluminescence backlight for better verification. It is theoretically available to protect the QDs within a strict environment by using encapsulation/printing, UV offset coating, organic/inorganic packaging and organic inorganic stacking. These packaging methods are suitable to encapsulate due to their high corrosion resistance, water vapor barrier properties, and thermal stability. As a kind of transparent fluid colloid, UV glue can fill the periphery of each QD to block the immersion path of moisture and vapor, and more importantly, the encapsulation by UV glue is easier to implement. Here, the DQDA layer was realized by screen printing method. The spherical CdSe QD material was bought from Poly Opto Electronics Co., Ltd, and the measured average diameter of a single QD is 10 nm. The QD slurry was prepared by dispersing QDs into toluene and printing ink. After that, the composite screen plate was fixed on a printing machine, and the QD slurry was spread on one side of the LGS. After lightly and vigorously scraping the QD slurry from one side to the other side on the screen plate, the QD slurry could be transferred from the mesh apertures to the substrate's surface due to the pressure. The LGS was then put into an oven under 50 °C through thermal curing for 15 min. Finally, the UV glue was spin coated on the DQDA layer followed by the barrier film attachment to ensure that the entire substrate was evenly covered by the UV glue.

After encapsulation, morphology characterization was evaluated under a fluorescence microscope (Olympus OLS4100). It is worth noting that certain encapsulation materials may lead to the quenching of QDs. As shown in Fig. 4(a), a large black spot can be observed on the QD surface. It indicates that the dissolution between the glue layer and DQDA occurred due to incompatibility among materials. What's more, the kind of damage of QD structure would affect the output light characteristics of uniformity and luminous brightness. The material used in our experiment were compatible with QDs, it would not cause the quenching after encapsulation. As can be seen from Fig. 4(b) and 4(c), the UV glue was specially chosen to effectively suppresses the dissolution. Fig. 4(b) and 4(c) are the morphology of the same DQDA before and after printing. The results show that the encapsulation of DQDA with our method will not affect the QD morphology and luminescent properties.

The optical performance was measured from nine-point measurement approach using a color luminance meter (SRC-200S) both before and after encapsulation. The testing points are drawn in Fig. 5. Before encapsulation, the maximum and lowest brightnesses are 4100 cd/m$^2$ and 3677 cd/m$^2$, respectively. After encapsulation, they slightly changed to 4299 cd/m$^2$ and 3353 cd/m$^2$,

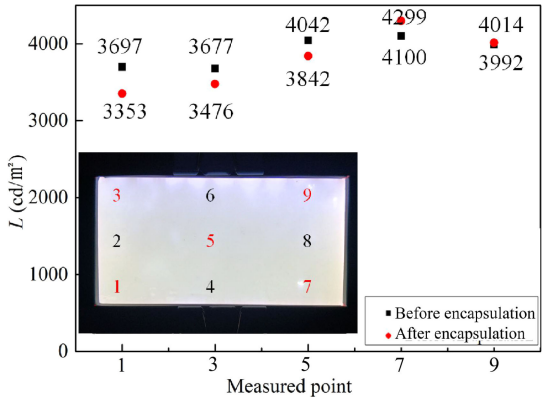


Fig. 5. The luminance comparison of the luminescent device before and after encapsulation (Inset is the encapsulated backlight prototype and the corresponding nine test positions).

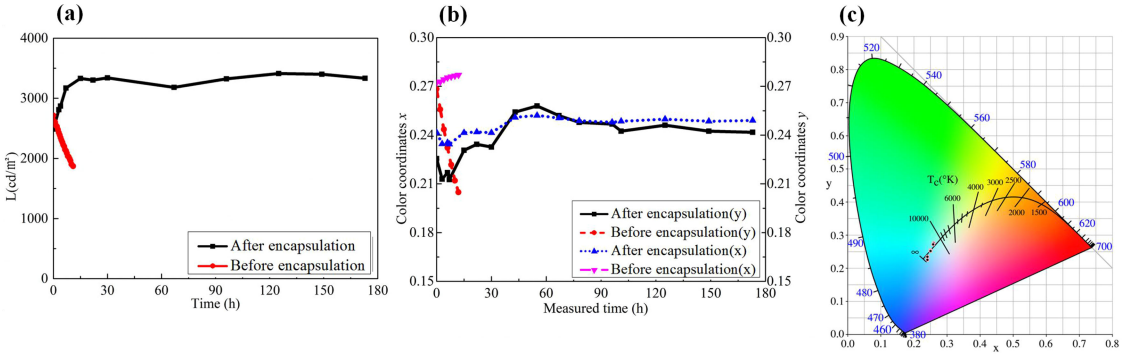


Fig. 6. Comparisons of the unencapsulated and encapsulated backlights at room temperature: the life aging results of (a) the luminance, (b) the chromaticity coordinates and (c) the changing trend of the chromaticity coordinates under CIE 1931 standard.

respectively. The uniformity of this luminescent device can be defined as the following formula:

$$U = \frac{L_{\min}}{L_{\max}} \tag{2}$$

where, $L_{\max}$ and $L_{\min}$ represent the maximum and the minimum values of the luminance, respectively. From Eq. (2), the uniformity before and after encapsulation decreases slightly from 89% to 78%. That is because the brightness at different point decreases or increase slightly, which can be seen in Fig. 5.

### *3.2 Life Aging at Room Temperature*

The unencapsulated and encapsulated devices were operated at room temperature. As shown in Fig. 6(a), the brightness of the unencapsulated device drops dramatically from 2714 cd/m$^2$ to 1872 cd/m$^2$ within 11 hours, while the brightness of the encapsulategd device remains stable over 170 hours. In addition, it is found that the brightness slightly increases from 2488 cd/m$^2$ to 3331 cd/m$^2$ during the life aging test. It is generally attributed to the transition of initial working state from a non-state to a steady state [44], [45]. As can be seen in Fig. 6(a), the initial 15 h can be considered as the non-steady state that the device brightness increases slightly. After that, the brightness becomes stable basically and reaches steady state. Therefore, the 15h point can

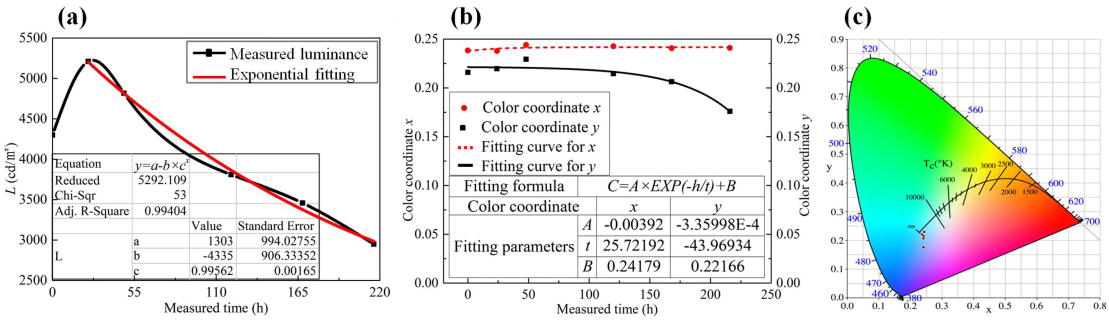


Fig. 7. The life aging results under 60 °C and 90% RH: (a) luminance changes within 216 hours. (b) the changing trend of the chromaticity coordinates x and y and (c) the changing trend of the chromaticity coordinates under CIE 1931 standard.

TABLE 2
The Changing Trend of Luminance and Chromaticity Coordinates

| Measured time (h) | 0 | 24 | 48 | 120 | 168 | 216 |
|---|---|---|---|---|---|---|
| Luminance (cd/m$^2$) | 4298.76 | 5210.33 | 4817.53 | 3810.27 | 3458.36 | 2949.67 |
| Coordinate x | 0.23834 | 0.23793 | 0.24405 | 0.24261 | 0.24068 | 0.24104 |
| Coordinate y | 0.21584 | 0.21968 | 0.22936 | 0.21459 | 0.2063 | 0.17604 |

be considered as the transition point between the two states. In terms of chromaticity coordinates shown in Fig. 6(b), the chromaticity coordinate y of the unencapsulated device drops 24% within 11 hours, while that of the encapsulated one keeps stable for a long time. The chromaticity coordinate x has the similar tend as the coordinate y. Fig. 6(c) is the changing trend of the chromaticity coordinates under CIE 1931 standard. These results show that this encapsulation method can improve the optical performance and provide the device long operation time at room temperature.

### 3.3 Life Aging in a High Temperature and Humidity Box

The encapsulated device was continuously operated in a high temperature and humidity box with the temperature of 60 °C and the humidity of 90% RH. The measured brightness began to rise to its peak in the first 55 hours, and then decreased from 5210.33 cd/m$^2$ to 4817.53 cd/m$^2$ with a downward trend. This trend can be fit by an exponential equation shown in Fig. 7(a). The subsequent trend meets the exponential fitting well, and the goodness of fit reaches over 0.99. It can be seen that the brightness attenuation of the became slower and slower after 120 hours. In terms of chromaticity coordinates shown in Fig. 7(b), the chromaticity coordinate x of the device kept stable for a long time under a harsh environment. However, the chromaticity coordinate y dropped 18% compared to the initial data. It can be also seen that the red QDs fail faster than the green QDs, but in general, they are within an acceptable range. These results show that this encapsulation method can improve the optical performance and provide the device long operation time at high temperature and humidity. However, it still has room to improve under a harsher environment.

## 4. Discussion

The mechanisms underlying the improved performance are discussed as following. The proposed encapsulation structure includes a UV glue layer and a barrier layer. During the fabrication process, the DQDA was fully solidified and dried before being encapsulated by the UV glue layer. The fluidity of the liquid UV glue can improve the surface defects and exhaust air from the DQDA. The UV glue also provides a heat conduction layer to dissipate heat from approaching the DQDA, and

preliminarily block the invasion of the environmental moisture and oxygen. The barrier layer can protect the DQDA and UV glue layer from physical damage, such as friction and squeezing. More importantly, the barrier layer with the thickness of 130 $\mu$m can provide perfect ability for isolating the environmental moisture and oxygen. By matching the refractive indices between the LGS and the UV glue layer, this stacked encapsulation structure does not change the original light path of the DQDA inside the LGS. The LED emitting rays are trapped inside the LGS due to the total reflection, and only when incident to the interface between the DQDA and the LGS, these rays will be extracted from the LGS after reflection by the reflective sheet. That means the output optical performance will not be affected by this encapsulation. Figure 5 shows that the brightness and the uniformity keep stable after encapsulation. The slight brightness change is mainly attributed to the improvement of surface defect or unevenness of the QD morphology. And it can be seen from Fig. 4 that this method will not cause deformation or collapse of the QD morphology. Therefore, the encapsulation of DQDA with our method will not affect the QD morphology and luminescent properties.

The encapsulation effect can be quantificationally analyzed by using the testing results of calcium film. The WVTR can only reach $10^{-2}$ (g/m$^2$/day) by using UV glue alone. However, the WVTR can be improved to $10^{-4}$ (g/m$^2$/day) in our encapsulation structure with a barrier film. It means that the ability to isolate moisture and oxygen has increased 100 times. At room temperature, the luminance of the unencapsulated device decreases by 24% within 11 hours. According to previous experience, this value can be equivalent to 5 times the room temperature, namely 1080 hours. That means the encapsulation effect has increased almost 100 times, which shows great matching with the results obtained by WVTR. In terms of chromaticity coordinates, the x coordinates of both devices are quite stable. However, the y coordinates of both devices show certain similar descent ratio. It indicates that the encapsulated device under a harsher environment still can keep for longer time than that at room temperature.

## 5. Conclusion

In this paper, we proposed a stacked encapsulation structure for DQDA to improve the lifetime and keep the optical performance stable for LCD backlight applications. This encapsulation structure provides an effective solution for discretely distributed QD devices. During this encapsulation, the DQDA was first fabricated by printing the QD slurry onto a LGS, and then coated with a thin UV glue layer and a barrier film. By specially optimizing the UV glue and barrier film, this ultra-thin encapsulation structure can improve the surface defects of the QD morphology without affecting the original light path and the output optical performance. The measured WVTR of this device is $1.29 \times 10^{-4}$ g/m$^2$/day, and the luminance can keep for over 1000 hours. More importantly, the lifetime of the encapsulated device is proved to be 100 times longer than that of the unencapsulated one. It is obvious that the stacked encapsulation structure can effectively prevent moisture and oxygen diffusion into the device from the atmosphere. This method also has potential to widely used for discrete structures in other device applications due to its easy fabrication process, high reliability, and low manufacturing costs.

## References

[1] L. Goldstein, F. Glas, J. Y. Marzin, and M. N. Charasse, "Growth by molecular beam epitaxy and characterization of InAs/GaAs strained-layer superlattices," *Appl. Phys. Lett.*, vol. 47, no. 10, pp. 1099–1101, 1985.
[2] A. P. Alivisatos, "Semiconductor clusters, nanocrystals and quantum dots," *Sci.*, vol. 271, no. 5251, pp. 933–937, 1996.
[3] H. Chen, J. H. Lee, B. Y. Lin, S. Chen, and S. T. Wu, "Liquid crystal display and organic light-emitting diode display: present status and future perspectives," *Light, Sci. Appl.*, vol. 7, 2018, Art. no. 17168.
[4] Z. Luo, D. Xu, and S. Wu, "Emerging quantum-dots-enhanced LCDs," *J. Display Technol.*, vol. 10, no. 7, pp. 526–539, 2014.
[5] B. Huang, T. Guo, S. Xu, Y. Ye, E. Chen, and Z. Lin, "Color converting film with quantum-dots for the liquid crystal displays based on inkjet printing," *IEEE Photon. J.*, vol. 11, no. 3, Jun. 2019, Art. no. 7000609.

[6] H. Kang *et al.*, "Color-by-blue QD-emissive LCD enabled by replacing RGB color filters with narrow-band GR InP/ZnSeS/ZnS QD films," *Adv. Opt. Materials*, vol. 6, no. 11, 2018, Art. no. 1701239.
[7] E. Chen *et al.*, "Flexible/curved backlight module with quantum-dots microstructure array for liquid crystal displays," *Opt. Exp.*, vol. 26, no. 3, pp. 3466–3482, 2018.
[8] S. Lin *et al.*, "Multi-primary-color quantum-dot down-converting films for display applications," *Opt. Exp.*, vol. 27, no. 20, 28480–28493, 2019.
[9] S. Coe-Sullivan, W. Liu, P. Allen, and J. S. Steckel, "Quantum dots for LED downconversion in display applications," *Ecs J. Solid Stateence, Technol.*, vol. 2, no. 2, pp. 3026–3030, 2013.
[10] S. H. Lee *et al.*, "Remote-type, high-color gamut white light-emitting diode based on InP quantum dot color converters," *Opt. Materials Exp.*, vol. 4, no. 7, 2014, Art. no. 1297.
[11] W. Song and H. Yang, "Efficient white-light-emitting diodes fabricated from highly fluorescent copper indium sulfide core/shell quantum dots," *Chemistry Materials*, vol. 24, no. 10, pp. 1961–1967, 2012.
[12] B. Geffroy, P. L. Roy, and C. Prat, "Organic light-emitting diode (OLED) technology: Materials, devices and display technologies," *Polym. Int.*, vol. 55, no. 6, pp. 572–582, 2010.
[13] W. Y. Wong, Z. He, S. K. So, K. L. Tong, and Z. Y. Lin, "A Multifunctional Platinum-Based Triplet Emitter for OLED Applications," *Organometallics*, vol. 24, no. 16, pp. 4079–4082, 2005.
[14] D. S. L. Alicia *et al.*, "Toward the minimization of fluorescence loss in hybrid cross-linked core-shell PS/QD/PMMA nanoparticles: Effect of the shell thickness," *Chem. Eng. J.*, vol. 313, pp. 261–269, 2017.
[15] K. Ferji *et al.*, "Fast and effective quantum-dots encapsulation and protection in PEO based photo-cross-linked micelles," *J. Colloid Interface Sci.*, vol. 476, pp. 222–229, 2016.
[16] A. Kumari, A. Sharma, U. Malairaman, and R. R. Singhet, "Proficient surface modification of CdSe quantum dots for highly luminescent and biocompatible probes for bioimaging: A comparative experimental investigation," *J. Lumin.*, vol. 199, pp. 174–182, 2018.
[17] W. Qi, Y. Wang, Z. Yu, B. Li, and L. Wu, "Fabrication of transparent and luminescent cdte/tio2 hybrid film with enhanced photovoltaic property," *Materials Lett.*, vol. 107, pp. 60–63, 2013.
[18] B. Zhao, Y. Yao, M. Gao, K. Sun, J. Zhang, and W. Li, "Doped quantum dot@ silica nanocomposites for white light-emitting diodes," *Nanoscale*, vol. 7, no. 41, pp. 17231–17236, 2015.
[19] H. Xie, E. Chen, Y. Ye, S. Xu, and T. Guo, "Highly stabilized gradient alloy quantum dots and silica hybrid nanospheres by core double shells for photoluminescence devices," *J. Phys. Chem. Lett.*, vol. 11, 1428–1434, 2020.
[20] Z. Li, W. Yao, L. Kong, Y. Zhao, and L. Li, "General method for the synthesis of ultrastable core/shell quantum dots by aluminum doping," *J. Amer. Chem. Soc.*, vol. 137, no. 29, pp. 12430–12433, 2015.
[21] S. Jun, J. Lee, and E. Jang, "Highly luminescent and photostable quantum dot–silica monolith and its application to light-emitting diodes," *Acs Nano*, vol. 7, no. 2, pp. 1472–1477, 2013.
[22] C. Yoon, H. J. Kim, M. H. Kim, K. Shin, Y. J. Kim, and K. Lee, "Fabrication of highly luminescent and concentrated quantum dot/poly (methyl methacrylate) nanocomposites by matrix-free methods," *Nanotechnol.*, vol. 28, no. 40, 2017, Art. no. 405203.
[23] Y. Xie *et al.*, "Synthesis of highly stable quantum-dot silicone nanocomposites via in situ zinc-terminated polysiloxane passivation," *Nanoscale*, vol. 9, no. 43, pp. 16836–16842, 2017.
[24] B. M. Hutchins, T. T. Morgan, M. G. Ucakastarlioglu, and M. E. Williams, "Optical properties of fluorescent mixtures: comparing quantum dots to organic dyes," *J. Chem. Educ.*, vol. 84, no. 8, pp. 1301–1303, 2007.
[25] A. J. Nozik, M. C. Beard, J. M. Luther, M. Law, and R. J. Ellingson, and J. C. Johnson, "Semiconductor quantum dots and quantum dot arrays and applications of multiple exciton generation to third-generation photovoltaic solar cells," *Chem. Rev.*, vol. 110, no. 11, pp. 6873–6890, 2010.
[26] P. M. Petroff and S. P. DenBaars, "MBE and MOCVD growth and properties of self-assembling quantum dot arrays in III-V semiconductor structures," *Superlattices Microstructures*, vol. 15, no. 1, pp. 15–20, 1994.
[27] S. H. Hu and X. Gao, "Stable Encapsulation of QD barcodes with silica shells," *Adv. Functional Materials*, vol. 20, no. 21, 2010, Art. no. 3721.
[28] J. J. Huang *et al.*, "Lifetime improvement of organic light emitting diodes using LiF Thin film and UV glue encapsulation," *Japanese J. Appl. Phys.*, vol. 47, no. 7, pp. 5676–5680, 2008.
[29] S. K. Kwak, T. W. Yoo, B. S. Kim, S. M. Lee, Y. S. Lee, and L. S. Park, "White LED packaging with layered encapsulation of quantum dots and optical properties," *Mol. Crystals Liquid Crystals*, vol. 564, no. 1, pp. 33–41, 2012.
[30] M. A. Hahn, P. C. Keng, and T. D. Krauss, "Flow cytometric analysis to detect pathogens in bacterial cell mixtures using semiconductor quantum dots," *Analytical Chemistry*, vol. 80, no. 3, pp. 864–872, 2008.
[31] W. Chung, K. Park, H. J. Yu, J. Kim, B. H. Chun, and S. H. Kim, "White emission using mixtures of CdSe quantum dots and PMMA as a phosphor," *Opt. Materials*, vol. 32, no. 4, pp. 515–521, 2010.
[32] Salerno and Mario, "Matter-wave quantum dots and antidots in ultracold atomic Bose-Fermi mixtures," *Phys. Rev. A*, vol. 72, no. 6, 2005, Art. no. 063602.
[33] C. Wang, S. Ni, S. Braun, M. Fahlman, and X. Liu, "Effects of water vapor and oxygen on non-fullerene small molecule acceptors," *J. Materials Chemistry C*, vol. 7, no. 4, pp. 879–886, 2019.
[34] W. J. Chia and Y. W. Chung, "Surface reaction studies of water and oxygen with polycrystalline Ni3Fe: evidence of water dissociation to produce hydrogen and its suppression by oxygen coadsorption," *Intermetallics*, vol. 4, no. 4, pp. 283–288, 1996.
[35] B. B. Stephens, P. S. Bakwin, P. P. Tans, R. M. Teclaw, and D. D. Baumann, "Application of a differential fuel-cell analyzer for measuring atmospheric oxygen variations," *J. Atmospheric Ocean. Technol.*, vol. 24, no. 1, pp. 82–94, 2007.
[36] M. Mazzeo *et al.*, "Organic single-layer white light-emitting diodes by exciplex emission from spin-coated blends of blue-emitting molecules," *Appl. Phys. Lett.*, vol. 82, no. 3, pp. 334–336, 2003.
[37] H. Zhang, H. Ding, M. J. Wei, C. Y. Li, B. Wei, and J. H. Zhang, "Thin film encapsulation for organic light-emitting diodes using inorganic/organic hybrid layers by atomic layer deposition," *Nanoscale Res. Lett.*, vol. 10, no. 1, pp. 1–5, 2015.

[38] S. Jun, J. Lee, and E. Jang, "Highly luminescent and photostable quantum dot–silica monolith and its application to light-emitting diodes," *ACS Nano*, vol. 7, no. 2, pp. 1472–1477, 2013.
[39] B. Dubertret, "In vivo imaging of quantum dots encapsulated in phospholipid micelles," *Sci.*, vol. 298, no. 5599, pp. 1759–62, 2002.
[40] B. I. Lemon and R. M. Crooks, "Preparation and characterization of dendrimer-encapsulated CdS semiconductor quantum dots," *J. Am. Chem. Soc.*, vol. 122, no. 51, pp. 12886–12887, 2015.
[41] D. Heitmann and J. P Kotthaus, "The spectroscopy of quantum dot arrays," *Phys. Today*, vol. 46, no. 6, pp. 56–63, 1993.
[42] R. Zhu, Z. Luo, H. Chen, Y. Dong, and S. T. Wu, "Realizing Rec 2020 color gamut with quantum dot displays," *Opt. Exp.*, vol. 23, no. 18, 2015, Art. no. 23680.
[43] M. Li, M. Xu, J. Zou, H. Tao, and J. Peng, "Realization of Al2O3/MgO laminated structure at low temperature for thin film encapsulation in organic light-emitting diodes," *Nanotechnol.*, vol. 27, no. 49, 2016, Art. no. 494003.
[44] S. A. Van Slyke, C. H. Chen, and C. W. Tang, "Organic electroluminescent devices with improved stability," *Appl. Phys. Lett.*, vol. 69, no. 15, 1996, Art. no. 2160.
[45] P. E. Burrows, V. Bulovic, S. R. Forrest, L. S. Sapochak, D. M. Mccarty, and M. E. Thompson, "Reliability and degradation of organic light emitting devices," *Appl. Phys. Lett.*, vol. 65, no. 23, 1994, Art. no. 2922.